Volume 23
Number 43
21 November 2025
Pages 9725-9982

Organic & Biomolecular Chemistry

rsc.li/obc

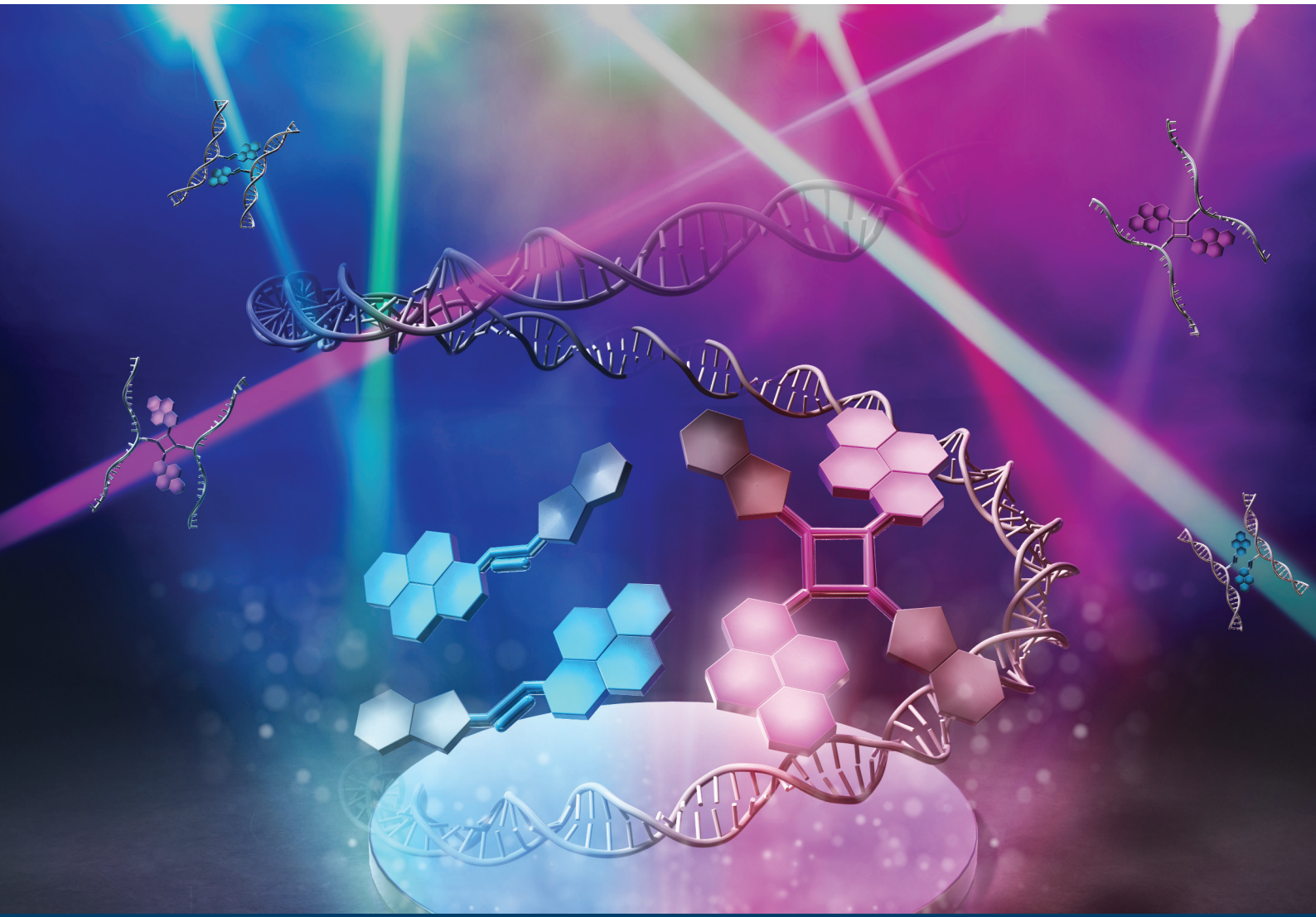

Themed issue: New Talent 2025

ISSN 1477-0520

ROYAL SOCIETY OF CHEMISTRY

PAPER
Keiji Murayama, Hiroyuki Asanuma *et al.*
Reversible photocycloaddition of 8-pyrenylvinylguanine for photoreactive serinol nucleic acid (SNA)

Organic & Biomolecular Chemistry

ROYAL SOCIETY OF CHEMISTRY

PAPER

View Article Online
View Journal | View Issue

Cite this: *Org. Biomol. Chem.*, 2025, **23**, 9862

Reversible photocycloaddition of 8-pyrenylvinylguanine for photoreactive serinol nucleic acid (SNA)†

Keiji Murayama, * Ayaka Ikeda, Fuminori Sato and Hiroyuki Asanuma *

Photoresponsive nanomachines are attractive components of functional nanodevices and nanosystems. To develop new photoresponsive nucleic acid-based nanomachines, we conjugated 8-pyrenylvinylguanine (^{PV}G) to a serinol linker and incorporated it into an acyclic xeno nucleic acid, serinol nucleic acid (SNA). The two ^{PV}G residues incorporated into SNA underwent interstrand photocycloaddition upon 447 nm light irradiation in the duplex state, whereas previously reported 8-pyrenylvinyladenine (^{PV}A) formed both intrastrand and interstrand photodimers. The ^{PV}G photodimer was converted to monomers by irradiation with 350 nm light. This photoreaction enabled reversible photoregulation of the formation and dissociation of the SNA/RNA duplex, although some byproducts were generated due to the slower photoreaction of ^{PV}Gs than that of ^{PV}As. In contrast, when a single ^{PV}G was incorporated into SNA, the interstrand photocycloaddition and cycloreversion were remarkably fast and effective in the single-stranded state. We utilized this to demonstrate a photocaging system that achieves one-way photoswitching of hybridization ability. The powerful photocycloaddition properties of ^{PV}G-SNA are expected to find applications in new photoresponsive nanodevices and nanosystems.

Received 4th June 2025,
Accepted 4th July 2025

DOI: 10.1039/d5ob00924c

rsc.li/obc

Introduction

DNA nanotechnology offers an attractive platform for realizing highly functional nanodevices and biological tools, such as DNA nanostructures,[1] DNA computing systems,[2] DNA-based nanomachines,[3] and molecular robotics.[4] Chemical modifications on nucleobases and additional incorporation of functional molecules into DNA strands facilitate the development of stimuli-responsive systems triggered by metal ions,[5] pH,[6] and photoirradiation,[7] providing powerful systems for the design of novel nanomachines based on nucleic acids.

To overcome the limitations of conventional DNA nanotechnology, it is essential to utilize xeno nucleic acids (XNAs)[8] with modified backbone structures that exhibit high resistance to enzymatic and chemical degradation and unique hybridization properties distinct from those of natural nucleic acids. In fact, several examples of nanotechnology utilizing XNAs have been reported, demonstrating greater functionality than those utilizing DNA.[9] We previously reported a reversible photoregulation of duplex formation and dissociation of serinol nucleic acid (SNA),[10] an acyclic XNA, by introducing two 8-pyrenylvinyladenine (^{PV}A) residues.[11] When blue light is irradiated onto the duplex composed of SNA containing two ^{PV}A residues and complementary RNA, a [2 + 2] photocycloaddition reaction occurs between the two ^{PV}A residues, causing the duplex to dissociate into single strands (Fig. 1A). On the other hand, upon UV light irradiation, the ^{PV}A photodimer undergoes photocycloreversion to regenerate monomeric ^{PV}A, enabling the re-formation of the duplex. This system shows promise for the development of photon-driven nanomachines and photocontrollable biological tools that use XNAs as building blocks. However, these strategies are limited to photoresponsive modification of the adenine base, requiring two adjacent adenines to design a photocontrollable system, which limits the range of applicable sequences.

We report on the photoregulation of SNA containing a photoresponsive nucleobase, 8-pyrenylvinylguanine (^{PV}G) (Fig. 1B). The synthesis of ^{PV}G incorporated into deoxyribose has already been reported.[12] Ogasawara demonstrated that ^{PV}G-modified DNA can be used as a photoswitch for G4 formation *via* the *trans–cis* isomerization of ^{PV}G, which was successfully applied to photoregulation of a transcription system.[13] We hypothesized that two adjacent ^{PV}G residues conjugated with a flexible SNA strand are more likely to cause a photocycloaddition than *cis*-isomerization as in the case of ^{PV}A, which should lead to a photoregulation system different

Graduate School of Engineering, Nagoya University, Furo-cho, Chikusa-ku, Nagoya 464-8603, Japan. E-mail: murayama@chembio.nagoya-u.ac.jp, asanuma@chembio.nagoya-u.ac.jp

† Electronic supplementary information (ESI) available: Supporting figures, NMR charts, and MALDI-TOF MS charts. See DOI: https://doi.org/10.1039/d5ob00924c

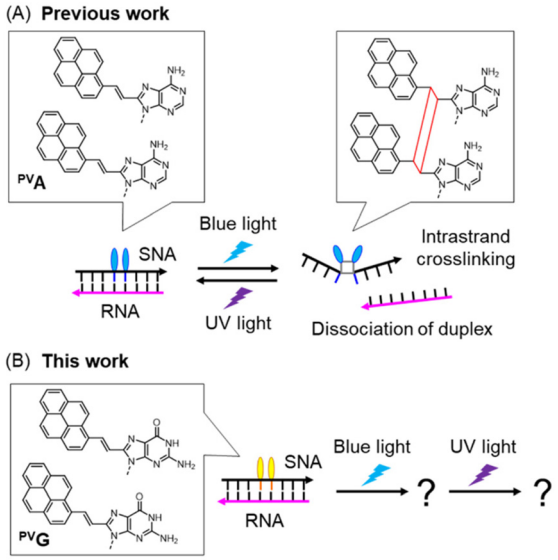

Fig. 1 Schematics of (A) previous work on the SNA strand modified with ^{PV}A residues and (B) this work on the SNA strand modified with ^{PV}G residues.

from the DNA-^{PV}G system based on a *trans–cis* isomerization. Therefore, we synthesized a novel ^{PV}G-SNA phosphoramidite monomer and incorporated it into the SNA strand, evaluated the photoreactivity of the ^{PV}G residue, and compared it with the ^{PV}A modification.

Results and discussion

Synthetic procedures for the ^{PV}G monomer

First, we prepared a phosphoramidite monomer of ^{PV}G-SNA according to Fig. 2. The *N*-9 position of 2-amino-6-chloropurine was converted to the benzyl ester form of compound **1**, and then the 6-position was substituted with oxygen to construct the guanine structure **3**. The formamidine protection on the 2-amino group resulted in an unexpected ester exchange from benzyl ester to ethyl ester **4**, but we continued the synthesis. After 8-bromination with NBS, the CuI/CsF-mediated Stille reaction[14] was carried out to obtain the 8-vinylguanine skeleton **6**. The Heck reaction with 1-bromopyrene followed by hydrolysis gave 2-protected-^{PV}G **8**. After coupling with DMTr-L-serinol, the desired phosphoramidite monomer **10** was successfully obtained using conventional phosphoramidite chemistry. The SNA strand with two ^{PV}G residues was synthesized using a DNA synthesizer, with each SNA monomer prepared as reported previously.[10]

Comparison of the photoreactivity between ^{PV}G and ^{PV}A introduced into the SNA strand

The melting temperature of the **SNA-2^{PV}G/RNA-2C** duplex was 40.4 °C (Fig. 3A), which is slightly higher than that of **SNA-2^{PV}A/RNA-2U** (31.0 °C, Fig. S1†). The stabilization of the duplex is probably caused by the strong stacking interaction of

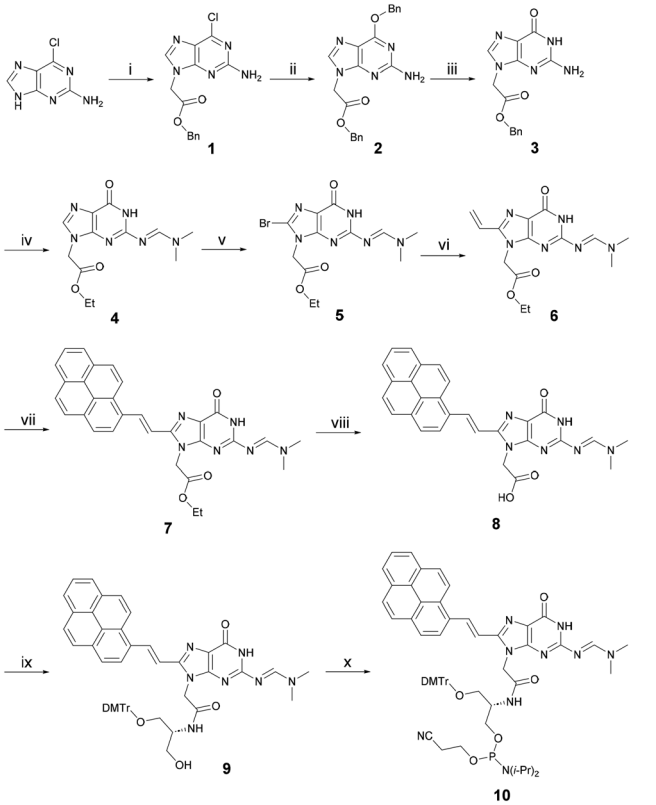

Fig. 2 Synthesis of a phosphoramidite monomer of ^{PV}G-SNA **10**. (i) Benzyl bromoacetate, DIPEA, DMF, 0 °C to r.t., and o.n., (ii) K_2CO_3, DABCO, benzyl alcohol, 80 °C, and 16 h, (iii) TFA, DCM, r.t., and 1 h, (iv) *N*,*N*-dimethylformamide diethyl acetal, EtOH, 50 °C, and 16 h, (v) NBS, DMF, r.t., and 2 h, (vi) $Pd(PPh_3)_4$, tributyl(vinyl)tin, CuI, CsF, DMF, 55 °C, and 4 h, (vii) 1-bromopyrene, $Pd(Ac)_2$, PPh_3, NEt_3, DMF, 110 °C, and 3 h, (viii) NaOH, 1,4-dioxane, MeOH, EtOH, H_2O, r.t., and 20 min, and (ix) DMTr-L-serinol, DMT-MM, NEt_3, DMF, and 0 °C for 20 min to r.t. for 1 h, and (x) 2-cyanoethyl *N*,*N*-diisopropylchlorophosphoramidite, NEt_3, CH_2Cl_2, 0 °C, and 30 min.

^{PV}Gs, as will be explained later. This result shows that **SNA-2^{PV}G** and **RNA-2C** form a duplex at room temperature, suggesting that the ^{PV}G substitution does not suppress duplex formation. Subsequently, the photoreactivity of ^{PV}G in the SNA strand was evaluated (Fig. 3). Upon 447 nm light irradiation of the **SNA-2^{PV}G/RNA-2C** duplex at 20 °C, the absorption band at around 400 nm decreased with the irradiation time, followed by the appearance of a new absorption band at around 330–360 nm, which was attributed to the pyrene moiety (Fig. 3B). The isosbestic points were 329 and 361 nm. This behavior is similar to the photocycloaddition of ^{PV}A residues in the **SNA-2^{PV}A/RNA-2U** duplex, indicating that ^{PV}G residues also form a photodimer *via* photocycloaddition rather than *cis*-isomerization under the same conditions (Fig. S2†).[12] When the photodimer of ^{PV}G was irradiated with 350 nm UV light, the absorption bands of the monomeric ^{PV}G were restored (Fig. 3C), indicating a cycloreversion reaction similar to that of ^{PV}A. We confirmed that pyrimidine dimers are not generated even when exposed to 350 nm light for 30 minutes under the

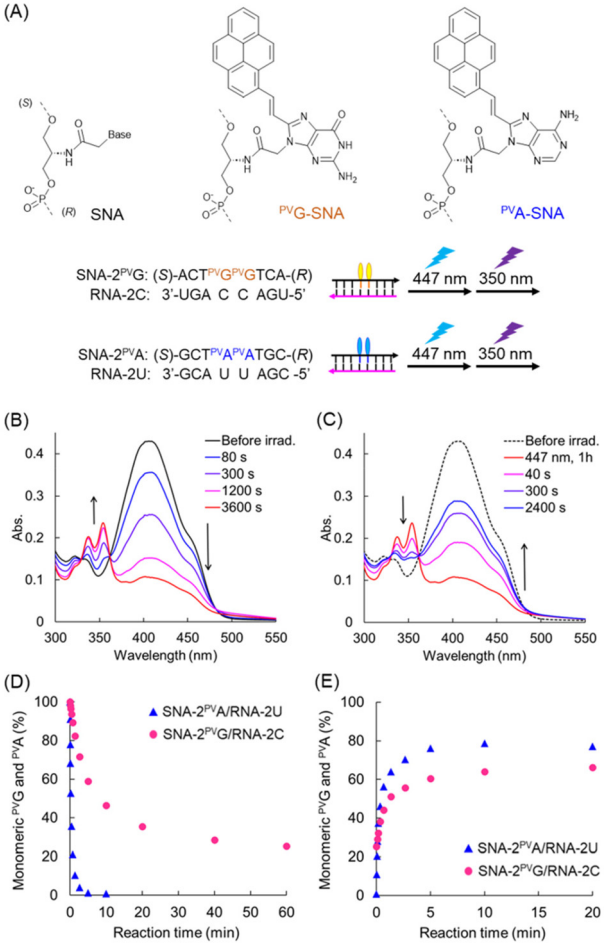

Fig. 3 (A) Chemical structures of SNA units, sequences used in this study, and schematics of the irradiation experiment. (B) Absorption spectra of **SNA-2^{PV}G/RNA-2C** before irradiation and at the indicated times of irradiation with 447 nm light. (C) Absorption spectra of **SNA-2^{PV}G/RNA-2C** before irradiation, after 1 h of irradiation with 447 nm and after irradiation for the indicated times with 350 nm light. Irradiation was performed at 20 °C. (D) and (E) The ratio of monomeric ^{PV}G in **SNA-2^{PV}G/RNA-2C** (purple circles) and that of monomeric ^{PV}A in **SNA-2^{PV}A/RNA-2U** (blue triangles, Fig. S2† for UV spectra) as a function of irradiation time: (D) with 447 nm light and (E) with 350 nm light. Before irradiation with 350 nm light, ^{PV}G and ^{PV}A were crosslinked by irradiation with 447 nm light for 1 h and 10 min, respectively. The ratio of the monomers was calculated from the absorbance at 400 nm.

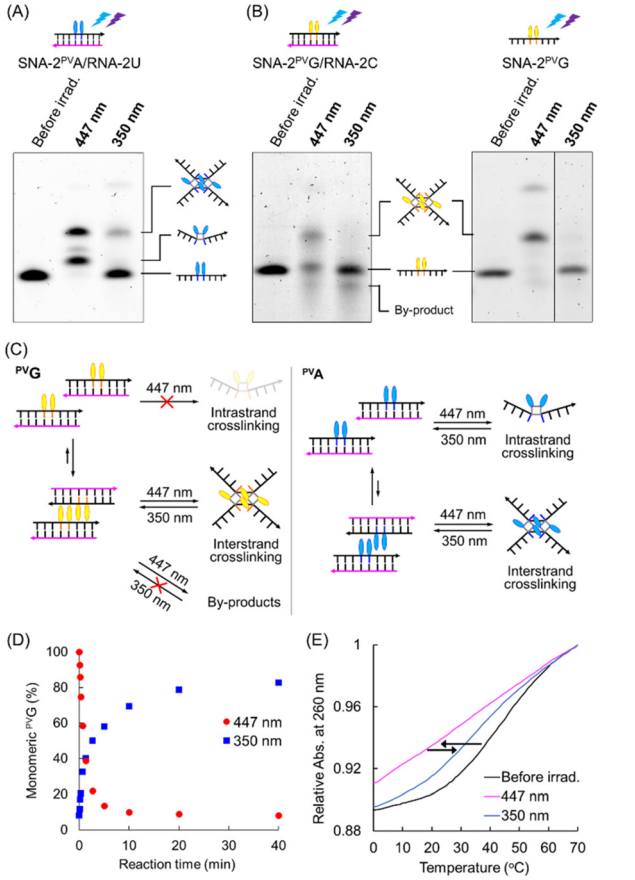

Fig. 4 (A) and (B) Gel-shift assay with denaturing PAGE. (A) **SNA-2^{PV}A/RNA-2U** duplex, (B, left) **SNA-2^{PV}G/RNA-2C** duplex, and (B, right) **SNA-2^{PV}G** single strand. The fluorescence of ^{PV}G and ^{PV}A was detected upon excitation using a 473 nm laser and a long-path filter (510 nm). (C) Illustration of different mechanisms of photocycloaddition between ^{PV}G and ^{PV}A. (D) The ratio of monomeric ^{PV}G in **SNA-2^{PV}G** single strands upon irradiation with 447 nm (red circles) and 350 nm (blue squares) light. (E) Melting profiles of **SNA-2^{PV}G/RNA-2C** before (black line) and after irradiation with 447 nm light (purple line) and 350 nm light (blue line).

present conditions (Fig. S12†). However, the kinetics of the photocycloaddition of **SNA-2^{PV}G/RNA-2C** were rather slow compared to **SNA-2^{PV}A/RNA-2U**: the half-life of the photodimerization of ^{PV}As was about 10 s (Fig. 3D), while that of ^{PV}Gs under the same conditions was over 10 min. Furthermore, the efficiency of cycloreversion also differed: 79% of the ^{PV}A photodimer was converted to monomers after 10 min of UV irradiation, whereas only 67% of the ^{PV}G photodimer was converted to monomers even after 30 min of UV irradiation (Fig. 3E).

To understand the reason for the different behavior of ^{PV}G and ^{PV}A, we performed denaturing PAGE analysis before and after light irradiation (Fig. 4A and B). To visualize the SNA strand, the entire gel was irradiated with 350 nm light after electrophoresis to restore the fluorescence of the monomeric ^{PV}G/^{PV}A and detected using an imaging analyzer with a blue laser. Note that both ^{PV}G and ^{PV}A are emissive upon blue light excitation. In the case of **SNA-2^{PV}A/RNA-2U**, irradiation with 447 nm light resulted in the appearance of two bands and the disappearance of the original band. The lower and the upper bands are assigned to the intrastrand and the interstrand crosslinking products, respectively (Fig. 4A). Under the present conditions employed, ^{PV}As were able to crosslink not only intrastrand but also interstrand. This fact suggests that a dimer of the **SNA-2^{PV}A/RNA-2U** duplexes is formed as an intermediate *via* association between ^{PV}As in the duplexes. Subsequent irradiation with 350 nm light significantly reduced these bands and regenerated the original band of **SNA-2^{PV}A** due to cycloreversion. In contrast, irradiation of **SNA-2^{PV}G/**

RNA-2C with 447 nm resulted in two additional bands in addition to the remaining unreacted **SNA-2^{PV}G** strand (Fig. 4B, left). The upper high-intensity band is attributed to the product of interstrand crosslinking because it showed significantly reduced mobility compared to intrastrand-crosslinked **SNA-2^{PV}A**. The lower band originated from unidentified by-products. Importantly, no band could be attributed to the intrastrand ^{PV}G-dimer, suggesting that intrastrand crosslinking of ^{PV}G was strongly suppressed. Upon irradiation with 350 nm light, the crosslinking product was converted to **SNA-2^{PV}G** with ^{PV}G monomers, whereas the by-products remained. Unlike **SNA-2^{PV}A/RNA-2U**, the **SNA-2^{PV}G/RNA-2C** duplex may facilitate a static stacking interaction between the interstrand ^{PV}Gs to form a dimer of the duplexes prior to photocrosslinking (Fig. 4C). In this case, it is difficult for ^{PV}G to adopt the necessary conformation for crosslinking, due to the rigid structure of the duplexes and the electrostatic repulsion between them.

This hypothesis was supported by the results of the irradiation experiments in the absence of complementary RNA. Irradiation with 447 nm light for single-stranded **SNA-2^{PV}G** showed significantly faster photocrosslinking than in the duplex state (Fig. 4D and Fig. S3†). The reaction half-life for photocycloaddition was approximately 1 min, which is about 10 times faster than that of the duplex state. The efficiency of the cycloreversion reaction for **SNA-2^{PV}G** was also improved: approximately 80% of the crosslinked ^{PV}G was converted to the monomer by irradiation with 350 nm light for 20 min. Denaturing PAGE revealed that the main product of photoirradiation on single-stranded **SNA-2^{PV}G** was also only the interstrand crosslinking product and that the formation of by-products was inhibited (Fig. 4B, right). The rapid photocycloaddition of single-stranded **SNA-2^{PV}G** can be explained by the fact that the single-stranded state facilitates the interaction between ^{PV}Gs on different strands due to the smaller electrostatic repulsion and that the flexibility of the single strand makes the dimerized structure of consecutive ^{PV}Gs suitable for photocrosslinking reactions compared to the rigid duplex state. As a result, the efficiency of cycloreversion was also enhanced due to the relative suppression of the irreversible side reaction during irradiation with 447 nm light. The concentration dependence of the photocrosslinking kinetics provided further evidence for the interstrand reaction of ^{PV}Gs. The crosslinking rate of 1 μM **SNA-2^{PV}G** with 447 nm light was found to be slower than that of 5 μM **SNA-2^{PV}G** (Fig. S3 and S4†). We conclude that two ^{PV}Gs introduced into the SNA strand undergo photocycloaddition reactions in an interstrand manner.

Although the reaction mechanism was different from what we expected, we hypothesized that the photoreaction of ^{PV}Gs would enable photoregulation of duplex formation. In **SNA-2^{PV}A/RNA-2U**, which induces both intrastrand and interstrand crosslinks, clear photoregulation of duplex formation and dissociation was observed, which was reversible and consistent with our previous results (Fig. S5†).[11] Irradiation of the **SNA-2^{PV}G/RNA-2C** duplex with 447 nm light at 20 °C led to the complete disappearance of the sigmoidal melting curve, indicating effective dissociation of the duplex by interstrand photocycloaddition of ^{PV}Gs (Fig. 4E, purple line). Upon irradiation of the photoadduct with 350 nm light, the sigmoidal curve partially recovered, supporting the re-formation of the duplex (Fig. 4E, blue line). However, ^{PV}G-SNA showed poor reversibility of the photoreaction (Fig. S6†), which is likely due to an unidentified by-product formed during the irradiation.

Although the precise mechanism remains unclear, it is postulated that ^{PV}G has a favorable orientation in photocycloaddition reactions, enabling it to photocrosslink solely *via* interstrand ^{PV}G dimerization (Fig. 4C). In addition, the strong stacking interaction between ^{PV}Gs facilitates interstrand association during the photoreaction (Fig. S7†). The formation of by-products could be the reason for the low cycloreversion efficiency of the ^{PV}G system compared to the ^{PV}A system.

Single ^{PV}G incorporated into the SNA strand for effective interstrand photocrosslinking

By focusing on the strong stacking property and selective interstrand photocycloaddition between ^{PV}Gs, we hypothesized that the SNA strand carrying a single ^{PV}G should undergo interstrand crosslinking and form a 4-arm branched SNA (Fig. 5A). We therefore prepared **SNA-1^{PV}G**, which carried only a single

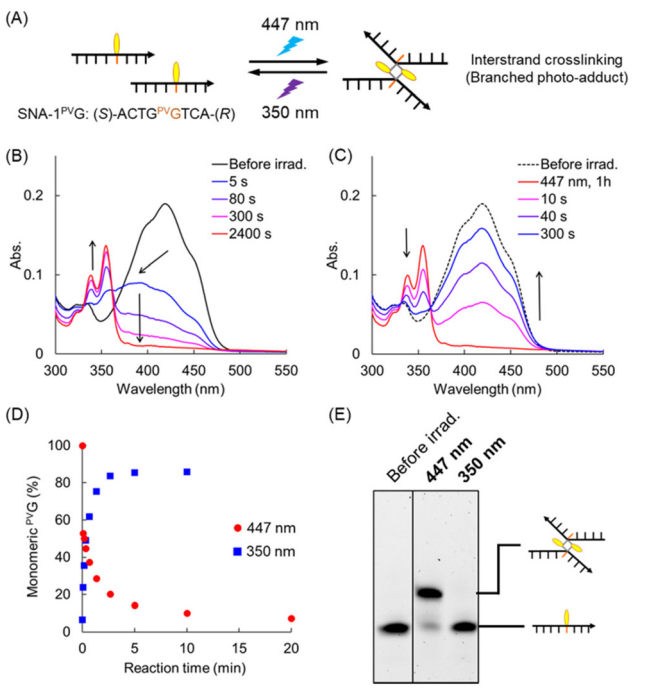

Fig. 5 (A) Schematic of the photoreaction of single-stranded **SNA-1^{PV}G** under light irradiation. (B) Absorption spectra of single-stranded **SNA-1^{PV}G** before and after irradiation for the indicated times with 447 nm light. (C) Absorption spectra of single-stranded **SNA-1^{PV}G** before irradiation, after 1 h of irradiation with 447 nm light and after irradiation for the indicated times with 350 nm light. Irradiation was performed at 20 °C. (D) The ratio of monomeric ^{PV}G in **SNA-1^{PV}G** single strands after irradiation at 447 nm (red circles) and 350 nm (blue squares). (E) Gel shift assay using denaturing PAGE before and after the light irradiation of the **SNA-1^{PV}G** single strand.

^{PV}G residue in the SNA strand, and recorded its absorption spectra after photoirradiation (Fig. 5B and C). Upon irradiation of single-stranded **SNA-1^{PV}G** with 447 nm light, a slight blue shift of the absorption band was observed, which was attributed to the *cis*-isomer of ^{PV}G. It subsequently disappeared with the appearance of the pyrene band (Fig. 5B). The isosbestic point was not observed. Presumably, ^{PV}G in **SNA-1^{PV}G** promotes rapid *trans*-to-*cis* isomerization of ^{PV}G, and *cis*-^{PV}G is also excited and reverted to the *trans* form, causing photocrosslinking upon irradiation with 447 nm light. **SNA-2^{PV}G** involving consecutive ^{PV}Gs probably suppresses *cis* isomerization through strong stacking interaction between ^{PV}Gs. The reaction rate of photocycloaddition for single stranded **SNA-1^{PV}G** was as fast as that for single-stranded **SNA-2^{PV}G** (Fig. 5D). Although *cis*-isomerization competed with photocrosslinking, the photocycloaddition reaction was remarkably fast. Fujimoto *et al.* reported that [2 + 2] photocycloaddition of 3-cyanovinylcarbazole (^{CNV}K) occurred only with the *trans* isomer.[15] In addition, the [2 + 2] photocycloaddition reaction is generally selective for *trans*-isomers.[16] We therefore hypothesize that *cis* ^{PV}G may also need to revert to the *trans* form prior to photocycloaddition (Fig. S8†). However, since some stilbene derivatives have been reported to undergo photodimerization between *trans*- and *cis*-isomers,[7h,17] it cannot be completely ruled out that the *cis*-^{PV}G may undergo a [2 + 2] photocycloaddition reaction. Upon irradiation of the photocrosslinked **SNA-1^{PV}G** with 350 nm light, the initial absorption band of ^{PV}G was rapidly restored, demonstrating that **SNA-1^{PV}G** underwent highly effective cycloreversion compared to **SNA-2^{PV}G** (Fig. 5C and D). Repeated irradiation experiments revealed that an effective photoreaction occurred for at least 5 cycles without severe photobleaching (Fig. S9†). Denaturing PAGE also confirmed the selective formation of the interstrand crosslinking product and the effective back reaction (Fig. 5E). The concentration dependence of the photoreaction confirmed an interstrand crosslinking reaction between ^{PV}Gs: the difference in kinetics between 1 μM and 5 μM was approximately fivefold (Fig. S10 and S11†).

Photocaging strategy of ^{PV}G-tethered SNA for the photoactivation of hybridization with RNA

We demonstrated the one-way photoswitching of the hybridization ability of **SNA-1^{PV}G** by photocycloreversion using the predimerized strand (Fig. 6A). The single-stranded **SNA-1^{PV}G** was irradiated with 447 nm light for 20 min to ensure complete photodimerization. Complementary RNA (**RNA-2C**) was then added, and the melting temperature was measured. The melting profile showed no transition, clearly indicating that the photocrosslinked **SNA-1^{PV}G** had lost its hybridization ability (Fig. 6B). After irradiating this sample with 350 nm light for 10 min, a sigmoidal curve was observed due to duplex formation. Thus, we confirmed that the photocaging strategy with pre-crosslinked **SNA-1^{PV}G** is feasible. We also confirmed that a single modification with ^{PV}A is applicable to the photocaging strategy (Fig. S13†).

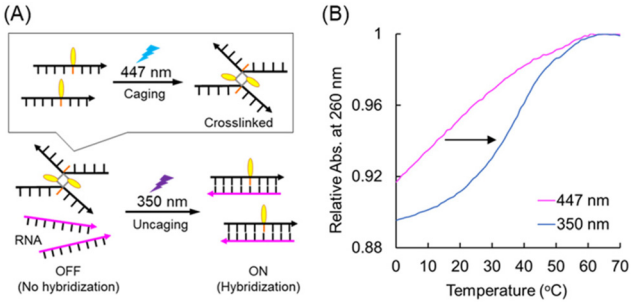

Fig. 6 (A) Schematic illustration of the photocaging strategy using the pre-crosslinked **SNA-1^{PV}G** dimer. (B) Melting profiles of the duplex of pre-crosslinked **SNA-1^{PV}G** and **RNA-2C** (purple line) and after irradiation with 350 nm light (blue line).

Experimental

Materials

Reagents for the synthesis of the ^{PV}G phosphoramidite monomer were purchased from Tokyo Kasei Co., Ltd, Wako Pure Chemical Industries, Ltd, and Aldrich. The reagents for oligomer synthesis and Poly-Pak II cartridges were purchased from Glen Research. The column for HPLC purification was purchased from Kanto Chemical Co., Ltd. RNA strands were purchased from Hokkaido System Science Co., Ltd.

Photoirradiation

447 nm light-emitting diodes (LEDs; CCS) and a xenon light source (MAX-301, Asahi Spectra) equipped with interference filters centered at 350 nm was used for photoirradiation. The sample solution was added to a cuvette, and the temperature during the light irradiation was controlled using a programmable temperature controller. All photoirradiation experiments were conducted at 20 °C.

Spectroscopic measurements

UV/vis spectra were measured using a JASCO model V-730 spectrometer equipped with a programable temperature controller; 10 mm quartz cells were used. The sample solutions contained 100 mM NaCl and 10 mM phosphate buffer (pH 7.0). The duplex concentration was 5.0 μM, and the experiments were performed in a 10 mm quartz cell.

Melting-temperature measurements

The melting curves of all nucleic acid duplexes were obtained using a JASCO model V-730 spectrometer equipped with a programable temperature controller by measuring the change in absorbance at 260 nm *versus* temperature. The melting curves for heating and cooling were recorded, and the average maximum value of their first derivatives was determined to be the melting temperature (T_m). The solution conditions were (unless otherwise noted) 100 mM NaCl, 10 mM phosphate buffer (pH 7.0), and 5.0 μM oligonucleotide.

Denaturing PAGE

Samples were loaded into the wells of a denaturing gel (20% acrylamide, 8 M urea, and 1 × TBE). Electrophoresis was performed at 4 W and r.t. for 2 h. The gels were irradiated with 350 nm light after electrophoresis to recover the fluorescence of the monomeric ^{PV}G and ^{PV}A. The gels were analyzed using a Typhoon FLA 9500 with a 473 nm laser and an LPB filter (510 nm).

Synthesis of compound 1. A suspended solution of 2-amino-6-chloropurine (5.00 g, 29.5 mmol) and *N*,*N*-diisopropylethylamine (5.53 mL, 32.5 mmol) in dry DMF was stirred in an ice bath for 10 min. Then, benzyl bromoacetate (5.55 g, 35.4 mmol) was added to the solution. After stirring for 1 h in an ice bath, stirring was done again at ambient temperature overnight. After evaporation, the residue was suspended in EtOH and filtered to collect the solid. The solid was washed with diethyl ether and dried *in vacuo* to afford **1** (6.77 g, 73%). ^{1}H-NMR [DMSO-d_6, 500 MHz] δ = 8.12 (s, 1H), 7.41–7.32 (m, 5H), 7.00 (s, 1H), 5.17 (s, 1H), 5.06 (s, 1H). ^{13}C-NMR [DMSO-d_6, 125 MHz] δ = 168.1, 160.4, 154.7, 149.9, 143.9, 135.8, 129.0, 128.8, 128.6, 123.4, 67.2, 44.5. HRMS (FAB) calcd for $C_{14}H_{12}ClN_5O_2$ (M + H$^+$): 318.0758. Found 318.0761.

Synthesis of compound 2. Under a N_2 atmosphere, benzyl alcohol (35 mL) was added to compound **1** (6.79 g, 21.4 mmol), K_2CO_3 (3.00 g, 21.4 mmol), and 1,4-diazabicyclo [2.2.2]octane (0.240 g, 2.14 mmol). The mixture was stirred at 80 °C for 16 h. After cooling to room temperature, chloroform was added to the mixture, which was then washed with water. The water layer was washed with chloroform, and the combined organic layer was subsequently washed with brine. The collected organic layer was evaporated. The residue was suspended with diethyl ether and then filtered to afford **2** as a solid (5.21 g, 63%). ^{1}H-NMR [DMSO-d_6, 500 MHz] δ = 7.86 (s, 1H), 7.52–7.31 (m, 10H), 6.53 (s, 1H), 5.50 (s, 1H), 5.18 (s, 2H), 5.01 (s, 2H). ^{13}C-NMR [DMSO-d_6, 125 MHz] δ = 168.4, 160.5, 160.3, 155.1, 140.6, 137.1, 135.9, 129.0, 128.9, 128.7, 128.54, 128.52, 113.7, 67.4, 67.1, 44.3. HRMS (FAB) calcd for $C_{21}H_{19}N_5O_3$ (M + H$^+$): 390.1566. Found 390.1560.

Synthesis of compound 3. Compound **2** (5.21 g, 13.4 mmol) was dissolved in a trifluoroacetate : CH_2Cl_2 = 1 : 1 solution and stirred for 1 h at room temperature. After brief evaporation, the residue was co-evaporated with acetonitrile three times. The residue was suspended in diethyl ether and then filtered to afford **3** as a solid (4.91 g, >100%). ^{1}H-NMR [DMSO-d_6, 500 MHz] δ = 10.88 (br, 1H), 7.88 (s, 1H), 7.40–7.32 (m, 5H), 6.72 (br, 1H), 5.19 (s, 1H), 4.97 (s, 1H). ^{13}C-NMR [DMSO-d_6, 125 MHz] δ = 167.8, 156.3, 154.3, 151.3, 137.9, 135.4, 128.6, 128.4, 128.1, 67.1, 44.5. HRMS (FAB) calcd for $C_{14}H_{13}N_5O_3$ (M + H$^+$): 300.1096. Found 300.1094.

Synthesis of compound 4. *N*,*N*-Dimethylformamide diethyl acetal (40 mL, 164 mmol) was added to compound **3** (4.91 g, 13.4 mmol), which was suspended in EtOH. The mixture was stirred for 16 h at 50 °C. After evaporation, it was re-precipitated by the addition of a small amount of cold ethyl acetate and then cooled in an ice bath. The precipitate was collected by filtration and dried *in vacuo* to afford **4** (2.67 g, 68%).^{1}H-NMR [DMSO-d_6, 500 MHz] δ = 11.29 (br, 1H), 8.52 (s, 1H), 7.79 (s, 1H), 4.95 (s, 2H), 4.17 (q, 2H), 3.13 (s, 3H), 3.02 (s, 3H), 1.22 (t, 3H). ^{13}C-NMR [DMSO-d_6, 125 MHz] δ = 168.5, 158.5, 158.1, 157.8, 150.6, 139.4, 119.3, 61.8, 44.2, 41.1, 35.1, 14.5. HRMS (FAB) calcd for $C_{12}H_{16}N_6O_3$ (M + H$^+$) 293.1362. Found 293.1343.

Synthesis of compound 5. Compound **4** (2.67 g, 9.13 mmol) was dissolved in dry DMF. *N*-Bromosuccinimide (1.96 g, 11.0 mmol) in dry DMF was added dropwise to the solution. The mixture was stirred for 2 h under a N_2 atmosphere. The reaction was quenched by the addition of 5% $Na_2S_2O_4$ aq. (dry DMF : 5% $Na_2S_2O_4$ aq. = 1 : 1) in an ice bath. After stirring for 5 min, the solution was extracted with chloroform and $Na_2S_2O_4$, and the organic layer was collected. The water layer was washed with chloroform. The combined organic layer was evaporated. The residue was suspended in small amounts of chloroform and large amounts of diethyl ether. The precipitate was collected by filtration and dried *in vacuo*, yielding **5** (3.11 g, 92%).^{1}H-NMR [DMSO-d_6, 500 MHz] δ = 11.46 (br, 1H), 8.59 (s, 1H), 4.91 (s, 2H), 4.20 (q, 2H), 3.15 (s, 3H), 3.03 (s, 3H), 1.23 (t, 3H). ^{13}C-NMR [DMSO-d_6, 125 MHz] δ = 167.6, 158.9, 158.2, 156.9, 151.9, 123.0, 119.6, 62.2, 44.7, 41.2, 35.2, 14.5. HRMS (FAB) calcd for $C_{12}H_{15}BrN_6O_3$ (M + H$^+$): 371.0467. Found 371.0482.

Synthesis of compound 6. Compound **5** (700 mg, 1.89 mmol), tetrakis(triphenylphosphine)palladium(0) (320 mg, 0.28 mmol), copper(I) iodide (70 mg, 0.38 mmol), and cesium fluoride (570 mg, 3.78 mmol) were suspended in dry DMF. Tributyl(vinyl)tin (1.1 mL, 3.78 mmol) was then added to the solution and the mixture was stirred at 55 °C for 4 h. The solution was filtered using Celite to remove the insoluble solid. After evaporation, the residue was purified by silica gel column chromatography ($CHCl_3$: MeOH = 20 : 1), yielding **6** (280 mg, 47%). ^{1}H-NMR [DMSO-d_6, 500 MHz] δ = 11.33 (s, 1H), 8.57 (s, 1H), 6.71 (m, 1H), 6.17 (s, 1H), 5.47 (d, 1H), 5.06 (s, 2H), 4.17 (q, 2H), 3.14 (s, 1H), 3.03 (s, 1H), 1.21 (t, 3H). ^{13}C-NMR [DMSO-d_6, 125 MHz] δ = 167.9, 158.2, 157.4, 157.2, 150.8, 145.3, 123.6, 119.5, 118.9, 61.5, 42.7, 40.7, 34.7, 14.0. HRMS (FAB) calcd for $C_{14}H_{18}N_6O_3$ (M + H$^+$) 319.1518. Found 319.1534.

Synthesis of compound 7. A solution of triphenylphosphine (66 mg, 0.22 mmol), palladium acetate (40 mg, 0.18 mmol), and triethylamine (1.05 mL) in dry DMF was stirred at 60 °C under a N_2 atmosphere until the color of the solution turned red. Then, 1-bromopyrene (320 mg 1.14 mmol) dissolved in dry DMF was added to the reaction mixture, followed by compound **6** (280 mg, 0.88 mmol) in dry DMF. The solution was refluxed at 110 °C for 3 h. The solution was filtered using Celite to remove the insoluble solid. After the evaporation, the residue was purified by silica gel column chromatography ($CHCl_3$: MeOH = 20 : 1) to afford **7** (220 mg, 48%). ^{1}H-NMR [DMSO-d_6, 500 MHz] δ = 11.42 (br, 1H), 8.74 (d, 1H), 8.65–8.10 (m, 10 H), 7.58 (d, 1H), 5.29 (s, 1H), 4.21 (s, 2H), 3.17 (s, 3H), 3.05 (s, 3H), 1.24 (t, 3H). ^{13}C-NMR [DMSO-d_6, 125 MHz] δ = 168.6, 158.6, 157.9, 157.6, 151.5, 146.6, 131.5, 131.4, 130.8,

130.5, 129.2, 128.7, 128.6, 128.2, 127.9, 127.0, 126.2, 125.9, 125.7, 124.8, 124.5, 124.3, 123.0, 120.1, 117.3, 61.9, 43.4, 41.2, 35.2, 14.5. HRMS (FAB) calcd for $C_{30}H_{26}N_6O_3$ (M + H^+): 519.2144. Found 519.2173.

Synthesis of compound 8. Sodium hydroxide (34 mg, 0.84 mmol) in a H_2O : EtOH = 1 : 1 solution was added to a stirred solution of compound **7** (220 mg, 0.42 mmol) in 1,4-dioxane : MeOH = 2 : 1 solution. The reaction mixture was stirred for 20 min at room temperature. After the addition of a large amount of H_2O, the pH was adjusted to 2–3 using 1 N HCl aq. The solid was collected by filtration using diethyl ether to afford **8** (150 mg, 86%). ^{1}H-NMR [DMSO-d_6, 500 MHz] δ = 11.63 (br, 1H), 8.86 (d, 1H), 8.73–8.79 (m, 10H), 7.62 (d, 1H), 5.22 (s, 1H), 3.19 (s, 3H), 3.06 (s, 3H). ^{13}C-NMR [DMSO-d_6, 125 MHz] δ = 169.1, 158.2, 157.5, 156.5, 150.5, 146.1, 131.4, 131.0, 130.3, 129.4, 128.5, 128.4, 127.4, 126.6, 125.9, 125.6, 125.3, 124.3, 123.9, 122.4, 118.1, 66.4, 43.2, 40.9. HRMS (FAB) calcd for $C_{28}H_{22}N_6O_3$ (M + H^+): 491.1831. Found 491.1836.

Synthesis of compound 9. To a stirred solution of compound **8** (0.15 g, 0.36 mmol) and triethylamine (three drops) dissolved in DMF, 1M DMTr-L-serinol[10] in DMF (0.33 mL, 0.33 mmol) was added. 4-(4,6-Dimethoxy-1,3,5-triazin-2-yl)-4-methylmorpholinium chloride (DMT-MM) (0.16 g, 0.50 mmol) was added to the solution at 0 °C, and stirred for 20 min at 0 °C, followed by an additional hour at room temperature. 20 mL of $CHCl_3$ was added to the solution and stirred for 10 min. The solution was extracted with $CHCl_3$ and sat. $NaHCO_3$ aq. twice. After evaporation, the residue was purified by silica gel column chromatography ($CHCl_3$: MeOH = 20 : 1, 1% triethylamine) to afford **9** (190 mg, 61%). ^{1}H-NMR [DMSO-d_6, 500 MHz] δ = 11.38 (br, 1H), 8.71–8.08 (m, 12H), 7.43–7.13 (m, 9H), 6.75 (m, 4H), 5.06 (dd, 2H), 4.81 (t, 1H), 4.07 (m, 1H), 3.642, 3.638 (s*2, 3H), 3.54 (m, 2H), 3.03 (m, 2H), 2.98 (s, 3H), 2.82 (s, 3H). ^{13}C-NMR [DMSO-d_6, 125 MHz] δ = 166.4, 157.93, 157.90, 157.5, 157.0, 151.3, 146.3, 145.0, 135.8, 135.7, 131.0, 130.8, 130.4, 130.1, 129.7, 129.6, 128.4, 128.2, 128.1, 127.73, 127.66, 127.4, 126.5, 125.7, 125.4, 125.2, 124.3, 124.1, 123.6, 122.5, 119.7, 117.2, 113.0, 85.2, 62.4, 60.8, 55.0, 54.9, 51.3, 44.3, 34.6. HRMS (FAB) calcd for $C_{52}H_{47}N_7O_6$ (M + H^+): 866.3666. Found 866.3697.

Synthesis of compound 10. Compound **9** (190 mg, 0.22 mmol) and triethylamine (0.13 mL, 1.1 mmol) were dissolved in dry dichloromethane under nitrogen. 2-Cyanoethyl diisopropylchlorophosphoramidite (70 μL, 0.33 mmol) was added dropwise to the solution at 0 °C. After stirring the mixture at room temperature for 30 min, it was subjected to silica gel column chromatography ($CHCl_3$: acetone = 3 : 1 containing 3% triethylamine). The products were then dissolved in a small amount of dry $CHCl_3$ and re-precipitated three times from hexane, yielding compound **10** (170 mg, 73%). Prior to synthesis of SNA using a DNA synthesizer, compound **10** was dried by co-evaporation with a mixture of dry acetonitrile and dry dichloromethane. ^{1}H-NMR [DMSO-d_6, 500 MHz] δ = 11.39 (br, 1H), 8.72–8.10 (m, 12H), 7.42–7.14 (m, 10H), 6.76 (m, 4H), 5.08 (d, 2H), 4.19 (m, 1H), 4.07 (m, 1H), 3.70–3.55 (m, 10H), 3.42 (m, 1H), 3.10 (m, 2H), 2.99, 2.98 (s*2, 3H), 2.83, 2.80 (s*2, 3H), 2.61 (m, 2H), 1.02 (m, 6H), 0.93 (m, 3H). ^{13}C-NMR [DMSO-d_6, 125 MHz] δ = 166.4, 158.0, 157.9, 157.8, 157.5, 157.0, 151.2, 146.3, 144.9, 135.6, 135.5, 131.0, 130.8, 130.4, 130.1, 129.7, 129.6, 128.4, 128.2, 128.1, 127.7, 127.6, 127.4, 126.5, 125.7, 125.4, 125.2, 124.3, 124.0, 123.5, 122.5, 119.7, 118.8, 117.3, 113.0, 85.2, 62.0, 58.2, 58.1, 54.9, 44.2, 42.4, 42.3, 34.6, 32.1, 29.6, 24.3, 24.2, 24.1, 19.8, 19.7. ^{31}P-NMR [DMSO-d_6, 202 MHz] δ = 146.9, 146.6. HRMS (FAB) calcd for $C_{61}H_{64}N_9O_7P$ (M + H^+) 1066.4744. Found 1066.4730.

Synthesis and purification of oligonucleotides

SNA phosphoramidite monomers involving T, G, A, and C were synthesized following reported procedures.[9] SNA oligomers (SNA-2^{PV}G and SNA-1^{PV}G) were synthesized using an NTS M-6-MX_A12N DNA/RNA synthesizer (Nihon Techno Service Co., Ltd) using phosphoramidite chemistry. For the coupling of all SNA monomers, the incubation time was extended to 600 s. The concentrations of the SNA phosphoramidite monomers were adjusted to 0.1 M for **10** (^{PV}G) and G, and 0.075 M for T, A, and C. **10** (^{PV}G) was dissolved in a dry CH_2Cl_2 : acetonitrile = 1 : 1 solution. The synthesized oligonucleotides were purified using Poly-Pak cartridges. The collected residue was further purified by reversed-phase HPLC (Kanto Chemical, Mightysil RP-18 GPII column). After purification, the synthesized oligonucleotides were characterized by MALDI-TOF MS. The preparation of SNA-2^{PV}A was described in a previous report.[11a]

Conclusions

We synthesized a ^{PV}G-linked SNA as a photoresponsive system. A previous report showed that ^{PV}A-SNA favored the formation of intrastrand photodimers upon irradiation with blue light. In contrast, ^{PV}G selectively formed interstrand photodimers at a slower reaction rate, likely due to the different orientation favouring photocycloaddition. The interstrand crosslinking and cycloreversion of **SNA-2^{PV}G/RNA-2C** enable the photoregulation of the dissociation and formation of duplexes upon light irradiation. The formation of by-products during irradiation of the **SNA-2^{PV}G/RNA-2C** duplex may prevent the photoreaction from being reversible. In contrast, the interstrand photocycloaddition and cycloreversion of single-stranded **SNA-1^{PV}G** were sufficiently fast and effective compared to the **SNA-2^{PV}G/RNA-2C** duplex. Ogasawara *et al.* reported a photoregulation system using the *trans–cis* photoisomerization of ^{PV}G-DNA, but the photocrosslinking property of ^{PV}G was not described.[12] The rigid cyclic structure of the DNA scaffold could suppress photocycloaddition, while the flexible acyclic SNA scaffold probably enables interstrand photocycloaddition with high efficiency. As we have demonstrated, effective and reversible interstrand crosslinking between ^{PV}Gs is useful as a component of photoreactive materials such as photocaging systems. In particular, ^{PV}G-SNA is a suitable candidate as a photocrosslinker for various materials that respond to visible light, instead of other photocrosslinkers,[18] because ^{PV}G-SNA facilitates effective inter-

molecular photocrosslinking even at μM concentrations due to strong stacking interactions. The powerful photocycloaddition properties of ^{PV}G-SNA promise applications in new photoresponsive nanodevices and advanced applications, such as chemical artificial intelligence.[19]

Author contributions

K. M. and H. A. conceived and designed the experiments. A. I. performed all experiments and F. S. supervised the organic syntheses. All authors analyzed the data, discussed the results, and co-wrote the manuscript.

Conflicts of interest

There are no conflicts to declare.

Data availability

The data supporting this article have been included as part of the ESI.†

Acknowledgements

This work was supported by the JST FOREST Program (JPMJFR2226, to K. M.); JSPS KAKENHI Grant Numbers JP20H05970, JP20H05968, JP23H00506, and JP25K00080 to K. M., and JP21H05025 to H. A.; and AMED (23am0401007 and 24ae0121056, to H. A.).

References

1 (*a*) N. C. Seeman, *J. Theor. Biol.*, 1982, **99**, 237; (*b*) P. W. K. Rothemund, *Nature*, 2006, **440**, 297; (*c*) Y. Ke, L. L. Ong, W. M. Shih and P. Yin, *Science*, 2021, **338**, 1177.

2 (*a*) L. M. Adleman, *Science*, 1994, **266**, 1021; (*b*) K. Sakamoto, H. Gouzu, K. Komiya, D. Kiga, S. Yokoyama, T. Yokomori and M. Hagiya, *Science*, 2000, **288**, 1223; (*c*) D. Y. Zhang and E. Winfree, *J. Am. Chem. Soc.*, 2009, **131**, 17303.

3 (*a*) C. Mao, W. Sun, Z. Shen and N. C. Seeman, *Nature*, 1999, **397**, 144; (*b*) B. Yurke, A. J. Turberfield, A. P. Mills, F. C. Simmel and J. L. Neumann, *Nature*, 2000, **406**, 605; (*c*) E. S. Andersen, M. Dong, M. M. Nielsen, K. Jahn, R. Subramani, W. Mamdouh, M. M. Golas, B. Sander, H. Stark, C. L. P. Oliveira, J. S. Pedersen, V. Birkedal, F. Besenbacher, K. V. Gothelf and J. Kjems, *Nature*, 2009, **459**, 73.

4 Y. Sato, Y. Hiratsuka, I. Kawamata, S. Murata and S. M. Nomura, *Sci. Rob.*, 2017, **2**, eaal3735.

5 (*a*) A. Ono and H. Togashi, *Angew. Chem., Int. Ed.*, 2004, **43**, 4300; (*b*) K. Tanaka, G. H. Clever, Y. Takezawa, Y. Yamada, C. Kaul, M. Shionoya and T. Carell, *Nat. Nanotechnol.*, 2006, **1**, 190; (*c*) J. Liu and Y. Lu, *Angew. Chem., Int. Ed.*, 2007, **46**, 7587; (*d*) S. Tanaka, K. Wakabayashi, K. Fukushima, S. Yukami, R. Maezawa, Y. Takeda, K. Tatsumi, Y. Ohya and A. Kuzuya, *Chem. – Asian J.*, 2017, **12**, 2388; (*e*) Y. Takezawa, K. Mori, W.-E. Huang, K. Nishiyama, T. Xing, T. Nakama and M. Shionoya, *Nat. Commun.*, 2023, **14**, 4759.

6 (*a*) T. Wada, N. Minamimoto, Y. Inaki and Y. Inoue, *J. Am. Chem. Soc.*, 2000, **122**, 6900; (*b*) D. Liu and S. Balasubramanian, *Angew. Chem., Int. Ed.*, 2003, **42**, 5734; (*c*) T. Ohmichi, Y. Kawamoto, P. Wu, D. Miyoshi, H. Karimata and N. Sugimoto, *Biochemistry*, 2005, **44**, 7125; (*d*) T. Li and M. Famulok, *J. Am. Chem. Soc.*, 2013, **135**, 1593; (*e*) A. Idili, A. Vallée-Bélisle and F. Ricci, *J. Am. Chem. Soc.*, 2014, **136**, 5836; (*f*) Y. Hu, C.-H. Lu, W. Guo, M. A. Aleman-Garcia, J. Ren and I. Willner, *Adv. Funct. Mater.*, 2015, **25**, 6867.

7 (*a*) X. Liang, H. Nishioka, N. Takenaka and H. Asanuma, *ChemBioChem*, 2008, **9**, 702; (*b*) Y. Yoshimura and K. Fujimoto, *Org. Lett.*, 2008, **10**, 3227; (*c*) S. Ogasawara and M. Maeda, *Angew. Chem., Int. Ed.*, 2008, **47**, 8839; (*d*) X. Wamg and X. Liang, *RSC Adv.*, 2016, **6**, 93398; (*e*) S. Mori, K. Morihiro and S. Obika, *Molecules*, 2014, **19**, 5109; (*f*) A. S. Lubbe, Q. Liu, S. J. Smith, J. W. Vries, J. C. M. Kistemaker, A. H. Vries, I. Faustino, Z. Meng, W. Szymanski, A. Herrmann and B. L. Feringa, *J. Am. Chem. Soc.*, 2018, **140**, 5069; (*g*) M. W. Haydell, M. Centola, V. Adam, J. Valero and M. Famulok, *J. Am. Chem. Soc.*, 2018, **140**, 16868; (*h*) A. M. Abdelhady, K. Onizuka, K. Ishida, S. Yajima, E. Mano and F. Nagatsugi, *J. Org. Chem.*, 2022, **87**, 2267; (*i*) L. Rieger, B. Pfeuffer and H.-A. Wagenknecht, *RSC Chem. Biol.*, 2023, **4**, 1037; (*j*) T. Anderson, W. Wu, O. Sirbu, K. Tong, S. Winna, X. R. Liu, B. Kou, K. Murayama, H. Asanuma and Z. Wang, *Angew. Chem., Int. Ed.*, 2024, **63**, e202405250; (*k*) T. Nakakuki, M. Toyonari, K. Aso, K. Murayama, H. Asanuma and T. de Greef, *ACS Synth. Biol.*, 2024, **13**, 521; (*l*) L. Wohlrábová, M. Sahlbach, A. Heckel and T. Slanina, *Chem. Commun.*, 2024, **60**, 4366; (*m*) M. Wakano, M. Tsunoda, K. Murayama, J. Morimoto, R. Ueki, S. Aoyama-Ishiwatari, Y. Hirabayashi, H. Asanuma and S. Sando, *J. Am. Chem. Soc.*, 2025, **147**, 11477.

8 (*a*) C. J. Leumann, *Bioorg. Med. Chem.*, 2002, **10**, 841; (*b*) J. C. Chaput and P. Herdewijn, *Angew. Chem., Int. Ed.*, 2019, **58**, 11570; (*c*) K. Murayama and H. Asanuma, *ChemBioChem*, 2021, **22**, 2507.

9 (*a*) U. Wenge and J. Wengel, *Angew. Chem., Int. Ed.*, 2012, **51**, 10026; (*b*) R. S. Zhang, E. O. McCullum and J. C. Chaput, *J. Am. Chem. Soc.*, 2008, **130**, 5846; (*c*) V. Kumar and V. Kesavan, *RSC Adv.*, 2013, **3**, 19330; (*d*) A. M. Kabza, B. E. Young and J. T. Sczepanski, *J. Am. Chem. Soc.*, 2017, **139**, 17715; (*e*) W.-C. Hsieh, G. R. Martinez, A. Wang, S. F. Wu, R. Chamdia and D. H. Ly, *Commun. Chem.*, 2018, **1**, 89; (*f*) M. K. Skaanning, J. Bønnelykke, M. A. D. Nijenhuis, A. Samanta, J. M. Smidt and K. V. Gothelf, *J. Am. Chem. Soc.*, 2024, **146**, 20141.

10 H. Kashida, K. Murayama, T. Toda and H. Asanuma, *Angew. Chem., Int. Ed.*, 2011, **50**, 1285.
11 (*a*) K. Murayama, Y. Yamano and H. Asanuma, *J. Am. Chem. Soc.*, 2019, **141**, 9485; (*b*) Y. Yamano, K. Murayama and H. Asanuma, *Chem. – Eur. J.*, 2021, **27**, 4599.
12 (*a*) S. Ogasawara and M. Maeda, *Nucleic Acids Symp. Ser.*, 2008, **52**, 369; (*b*) Y. Saito, K. Matsumoto, Y. Takeuchi, S. S. Bag, S. Kodate, T. Morii and I. Saito, *Tetrahedron Lett.*, 2009, **50**, 1403.
13 S. Ogasawara, *ACS Synth. Biol.*, 2018, **7**, 2507.
14 S. P. H. Mee, V. Lee and J. E. Baldwin, *Angew. Chem., Int. Ed.*, 2004, **43**, 1132.
15 K. Fujimoto, A. Yamada, Y. Yoshimura, T. Tsukaguchi and T. Sakamoto, *J. Am. Chem. Soc.*, 2013, **135**, 16161.
16 (*a*) M. S. Syamala and V. Ramamurthy, *J. Org. Chem.*, 1986, **51**, 3712; (*b*) H. Meier, *Angew. Chem., Int. Ed. Engl.*, 1992, **31**, 1399; (*c*) F. D. Lewis, T. Wu, E. L. Burch, D. M. Bassani, J.-S. Yang, S. Schneider, W. Jager and R. L. Letsinger, *J. Am. Chem. Soc.*, 1995, **117**, 8785; (*d*) W. Herrmann, S. Wehrle and G. Wenz, *Chem. Commun.*, 1997, 1709; (*e*) B. Juskowiak and M. Chudak, *Photochem. Photobiol.*, 2004, **79**, 137; (*f*) M. Schraub, H. Gray and N. Hampp, *Macromolecules*, 2011, **44**, 8755; (*g*) O. A. Fedorova, A. E. Saifutiarova, E. N. Gulakova, E. O. Guskova, T. M. Aliyeu, N. E. Shepel and Y. V. Fedorov, *Photochem. Photobiol. Sci.*, 2019, **18**, 2208; (*h*) J. Seylar, D. Stasiouk, D. L. Simone, V. Varshney, J. E. Heckler and R. McKenzie, *RSC Adv.*, 2021, **11**, 6504; (*i*) T. P. Martyanov, A. P. Vorozhtsov, N. A. Aleksandrova, I. V. Sulimenkov, E. N. Ushakov and S. P. Gromov, *ACS Omega*, 2022, **7**, 42370.
17 (*a*) D. M. Bassani, X. Sallenave, V. Darcos and J.-P. Desvergne, *Chem. Commun.*, 2001, 1446; (*b*) H. Maeda, R. Hiranabe and K. Mizuno, *Tetrahedron Lett.*, 2006, **47**, 7865; (*c*) C. T. Eckdahl, C. Ou, S. Padgaonkar, M. C. Hersam, E. A. Weiss and J. A. Kalow, *Org. Biomol. Chem.*, 2022, **20**, 6201; (*d*) V. X. Truong and C. Barner-Kowollik, *Aust. J. Chem.*, 2022, **75**, 899.
18 (*a*) J. Zhang, S.-X. Tang, R. Fu, X.-D. Xu and S. Feng, *J. Mater. Chem. C*, 2019, **7**, 13786; (*b*) K. Kalayci, H. Frisch, C. Barner-Kowollik and V. X. Truong, *Adv. Funct. Mater.*, 2020, **30**, 1908171; (*c*) K. Kalayci, H. Frisch, V. X. Truong and C. Barner-Kowollik, *Nat. Commun.*, 2020, **11**, 4193; (*d*) J. Bai, Z. Shi, X. Ma, J. Yin and X. Jiang, *Macromol. Rapid Commun.*, 2022, **43**, 2200055; (*e*) R. T. Michenfelder, L. Delafresnaye, V. X. Truong, C. Barner-Kowollik and H.-A. Wagenknecht, *Chem. Commun.*, 2023, **59**, 4012; (*f*) D. Hoenders, S. Ludwanowski, C. Barner-Kowollik and A. Walther, *Angew. Chem., Int. Ed.*, 2024, **63**, e202405582; (*g*) C. Dohmen and H. Ihmels, *ChemPhotoChem*, 2024, **8**(7), e202300318.
19 (*a*) S. Murata, T. Toyota, S. I. M. Nomura, T. Nakakuki and A. Kuzuya, *Adv. Funct. Mater.*, 2022, **32**, 2201866; (*b*) A. Kuzuya, S. I. M. Nomura, T. Toyota, T. Nakakuki and S. Murata, *IEEE Trans. Mol. Biol. Multi-Scale Commun.*, 2023, **9**, 354.